EPJ Web of Conferences **67**, 02090 (2014)
DOI: 10.1051/epjconf/20146702090

Comparison of pool boiling heat transfer for different tunnel-pore surfaces

Robert Pastuszko[1,a]

[1]Kielce University of Technology, Department of Mechanics, Al. Tysiaclecia P.P.7, 25-314 Kielce, Poland

Abstract. Complex experimental investigations of boiling heat transfer on structured surfaces covered with perforated foil were performed. Experimental data were discussed for three kinds of enhanced surfaces: tunnel structures (TS), narrow tunnel structures (NTS) and mini-fins with the copper wire net (NTS-L). The experiments were carried out with water, ethanol, R-123 and FC-72 at atmospheric pressure. The TS and NTS surfaces were manufactured out of perforated copper foil (hole diameters: 0.3, 0.4, 0.5 mm) sintered with the mini-fins, formed on the vertical side of the 5 and 10 mm high rectangular main fins and horizontal inter-fin surface. The NTS-L surfaces were formed by mini-fins of 0.5 and 1 mm height uniformly spaced on the base surface. The wire mesh with an aperture of 0.32, 0.4 and 0.5 mm sintered with the fin tips formed a system of connected perpendicular horizontal tunnels. The tunnel width was 0.6 – 1.0 – 1.5 mm and the depth was 0.5 or 1.0 mm. The effects of the Bond number and dimensionless parameters for three kinds of enhanced structures on heat transfer ratio at nucleate pool boiling were examined.

1 Introduction

Boiling heat transfer enhancement is effective provided that specific surfaces are used (*enhanced boiling surfaces*). The studies conducted since the 1960s at numerous research centers have shown that the most efficient method of increasing the density of the heat flux and the value of the heat transfer coefficient is the use of coverings that are either porous or porous and capillary, the employment of enhanced surfaces or forming the channels, tunnels and hollows/cavities linked with the surface by a narrow „outlet". The following factors facilitate boiling heat transfer intensification:

- artificially produced nucleation sites in the form of pores contribute to the increase in the nucleation site densities,
- increasing the wetted surface by using the tunnels/channels and additionally extending the surface through the use of the fins/mini-fins/micro-fins,
- film vaporization or vaporization from the menisci in the subsurface tunnels/hollows/cavities,
- internal convection associated with the liquid flow in the tunnels/channels, forced by the capillary forces and the pumping action of the growing bubbles,
- external convection associated with the growth, departure and movement of the vapor bubbles.

This article summarizes the results of the boiling heat transfer investigations conducted on three types of surfaces with subsurface tunnels. The measurement data for the four types of working fluid used in the studies were taken from [1,2,3,4].

2 Experimental research

2.1 Investigated surfaces

2.1.1 TS surfaces

The specimens with the tunnel structures (TS) formed a square with sides of length 27 mm (w_f). The three main fins comprising the square were modified to include tunnels on the vertical surfaces and in the horizontal inter-fin spaces. The perforated copper foil was sintered to the machined surfaces (figure 1) creating a structure of combined U-shaped tunnels with the following parameters:

- fin number: 3,
- fin height: 5 and 10 mm (h_f),
- fin thickness: 5 mm (δ_f),
- inter-fin space width: 5 mm (s),
- tunnel depth: 1.6 mm (h_{tun}),
- tunnel width: 1.3 mm (w_{tun}),

[a] Corresponding author: tmprp@tu.kielce.pl

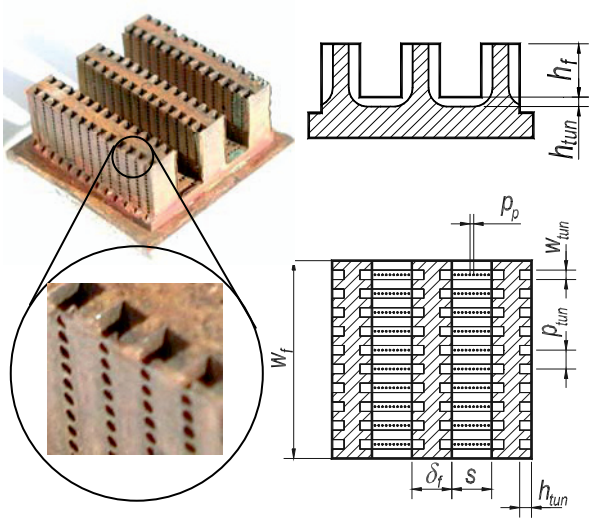

a) b)

Fig. 1. Investigated TS surfaces: a) views of the specimen with 10 mm high fins, b) cross sections.

- tunnel pitch: 2.0 – 2.25 – 2.5 mm (p_{tun}),
- pore diameter: 0.3 – 0.4 – 0.5 mm (d_p),
- pore pitch: 0.6 – 0.8 – 1.0 mm (p_p=2d_p).

2.1.2 NTS surfaces

The main fins were thru-milled to form mini-fins with the width corresponding to the thickness of the base fins. Additionally, an array of combined tunnels was created, closed with the sintered perforated foil or the wire mesh. The parameters of the NTS specimens were as follows (figure 2):

- fin number: 3,
- fin height: 5 and 10 mm (h_f),
- fin thickness: 5 mm (δ_f),
- inter-fin space width: 5 mm (s),
- tunnel depth in inter-fin spaces: 1.0 mm (h_{tunH}),
- tunnel width: 0.6 – 1.0 – 1.5 mm (w_{tun}),
- tunnel pitch: 2.0 mm (p_{tun}),
- pore diameter: 0.3 – 0.4 – 0.5 mm (d_p),
- pore pitch: 0.6 – 0.8 – 1.0 mm (p_p=2d_p).

2.1.3 NTS-L surfaces

These are the structural surfaces formed by sintering the woven copper wire mesh made of wire 0.14; 0.2; 0.32 mm in diameter to the mini-fin tips. The copper specimens, square in shape with a side of 26,5 mm, had 112 mini-fins and formed a system of tunnels intersecting at 90 degrees (figure 3).

Measurements were conducted also for NTS-L surfaces without a sintered wire mesh (plain mini-fins). The following parameters are used (figure 3):

- mini-fin number: 112,
- mini-fin height: 0.5 and 1.0 mm (h_f),
- mini-fin thickness: 2 mm (δ_f),

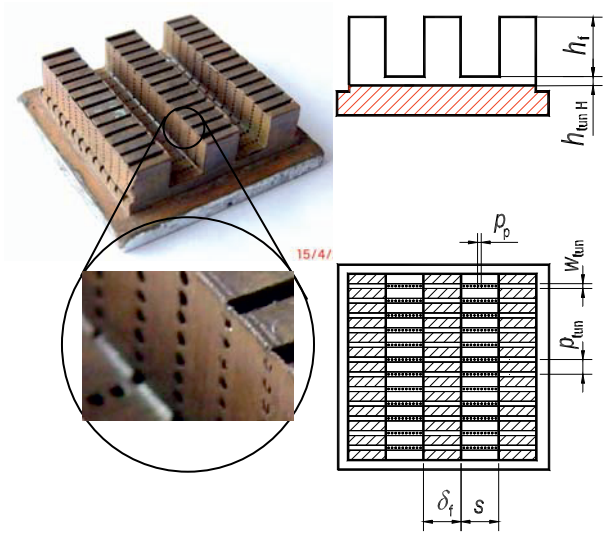

a) b)

Fig. 2. Investigated NTS surfaces: a) views of the specimen with 5 mm high fins, b) cross sections.

- inter-mini-fin space width: 1.5 mm (s),
- tunnel depth in inter-fin spaces: 0.5/1.0 mm (h_f),
- tunnel width: 0.6 – 1.0 – 1.5 mm (w_{tun}),
- tunnel pitch: 2.0 mm (p_{tun}),
- wire mesh: 0.32 – 0.4 – 0.5 mm (a),
- pore pitch: 0.6 – 0.8 – 1.0 mm (p_p=2d_p).

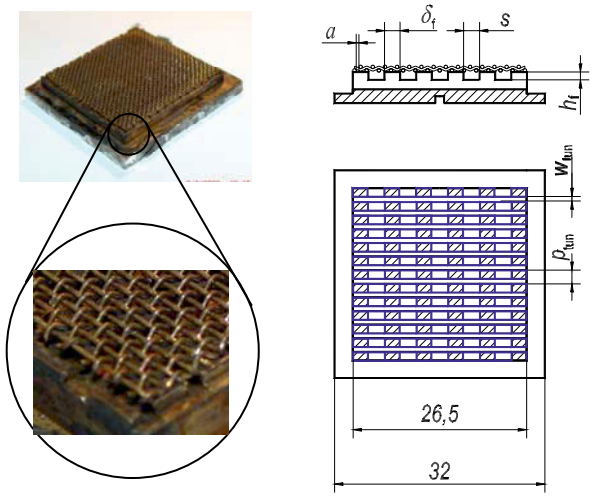

a) b)

Fig. 3. Investigated NTS-L surfaces: a) views of the specimen, b) cross sections.

2.2 Experimental set-up

The experimental set-up designed for determining the boiling curves and heat transfer coefficients was composed of the following modules (figure 4):

A. the basic module interchangeable with the module for internal visualization;
B. the power module and the supplied electric power measurement;
C. the temperature measurement and data acquisition module;

D. the vapor cooling and condensate recovery module.

The set-up had two test tracks facilitating independent measurements on two surfaces.

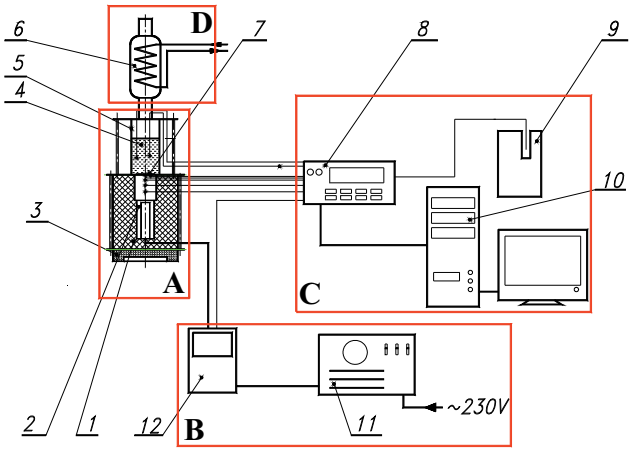

Fig. 4. Measuring apparatus: 1 – insulation; 2 – copper bar with cartridge heater; 3 – Teflon casing; 4 – boiling liquid; 5 – glass vessel; 6 – condenser; 7 – investigated sample; 8 – data logger & acquisition system; 9 – dry-well calibrator; 10 – PC; 11 – power supply (transformer and fuses); 12 – wattmeter.

Selected thermodynamic parameters of four working fluids used in the experiments, at the saturation temperature, are summarized in table 1.

Table 1. Thermodynamic parameters of saturated fluids [5,6].

Parameters at p=101.3 kPa	**Water**	**Ethanol**	**FC-72**	**R-123**
T_{sat}, ^{0}C	100	78.3	56.4	27.5
ρ_l, kg/m^3	959	757	1602	1457
ρ_v, kg/m^3	0.597	1.43	13.24	6.39
μ_l, Pa s	$2.8\cdot10^{-4}$	$4.4\cdot10^{-4}$	$4.3\cdot10^{-4}$	$4.1\cdot10^{-4}$
c_{pl}, J/kgK	4220	723	1103	1023
i_{lv}, kJ/kg	2251	963	94.9	170
λ_l, W/mK	0.68	0.169	0.055	0.077
σ_l, N/m	0.0589	0.0177	0.0081	0.015
L, mm	2.5	1.55	0.72	1.03

3 Results

3.1 Bond number

The Bond number is the ratio of characteristic dimension to capillary length. For TS or NTS surfaces:

$$\mathrm{Bo_d} = \left(\frac{d_\mathrm{p}}{L}\right)^2 \tag{1}$$

and for NTS-L surface:

$$\mathrm{Bo_a} = \left(\frac{a}{L}\right)^2 \tag{2}$$

where:

d_p – pore diameter, m

a – mesh aperture dimension, m.

The capillary length L characterizes potential for bubble departure and coalescence:

$$L = \sqrt{\frac{\sigma}{g(\rho_l - \rho_v)}} \tag{3}$$

where:

ρ_l – saturated liquid density, kg/m^3

ρ_v – saturated vapor density, kg/m^3

σ – surface tension, N/m.

It is proportional to vapor bubble departure diameter.

3.2 Generalized results

The measurement data collected help to generalize the results in the form of the dependence of the selected surface heat transfer coefficient/smooth flat surface coefficient ratio on the Bond number and varying geometric parameters:

- TS surface:

$$\frac{\alpha}{\alpha_s} = \mathrm{f}\left(\mathrm{Bo_d}^{0,5}\frac{p_\mathrm{tun}}{h_\mathrm{f}}\right) = \mathrm{f}\left(\frac{d_\mathrm{p}}{L}\frac{p_\mathrm{tun}}{h_\mathrm{f}}\right) \tag{4}$$

- NTS surface:

$$\frac{\alpha}{\alpha_s} = \mathrm{f}\left(\mathrm{Bo_d}^{0,5}\frac{w_\mathrm{tun}}{h_\mathrm{f}}\right) = \mathrm{f}\left(\frac{d_\mathrm{p}}{L}\frac{w_\mathrm{tun}}{h_\mathrm{f}}\right) \tag{5}$$

- NTS-L surface:

$$\frac{\alpha}{\alpha_s} = \mathrm{f}\left(\mathrm{Bo_a}^{0,5}\frac{w_\mathrm{tun}}{h_\mathrm{f}}\right) = \mathrm{f}\left(\frac{a}{L}\frac{w_\mathrm{tun}}{h_\mathrm{f}}\right) \tag{6}$$

where:

α – heat transfer coefficient for the surfaces: TS/NTS/NTS-L, W/m^{2}K

α_s – heat transfer coefficient for smooth surfaces, W/m^{2}K

p_tun – tunnel pitch, m

w_tun – tunnel width, m

h_f – fin/mini-fin height, m.

The relevant graphs are presented in figures 5 – 7. The horizontal strips denote the ranges of optimal parameters for particular working fluids. The boiling heat transfer coefficients for the smooth surfaces were determined on the basis of the power-law approximation of data from own measurements in the

form of the dependence of the heat transfer coefficient on the heat flux:

- water: $\alpha = 0.34\ q^{0.67}$,
- ethanol: $\alpha = 0.133\ q^{0.8}$,
- R-123: $\alpha = 0.24\ q^{0.6}$.

For FC-72 the dependence $\alpha = 0.3\ q^{0,66}$ was calculated on the basis of data found in the literature [7].

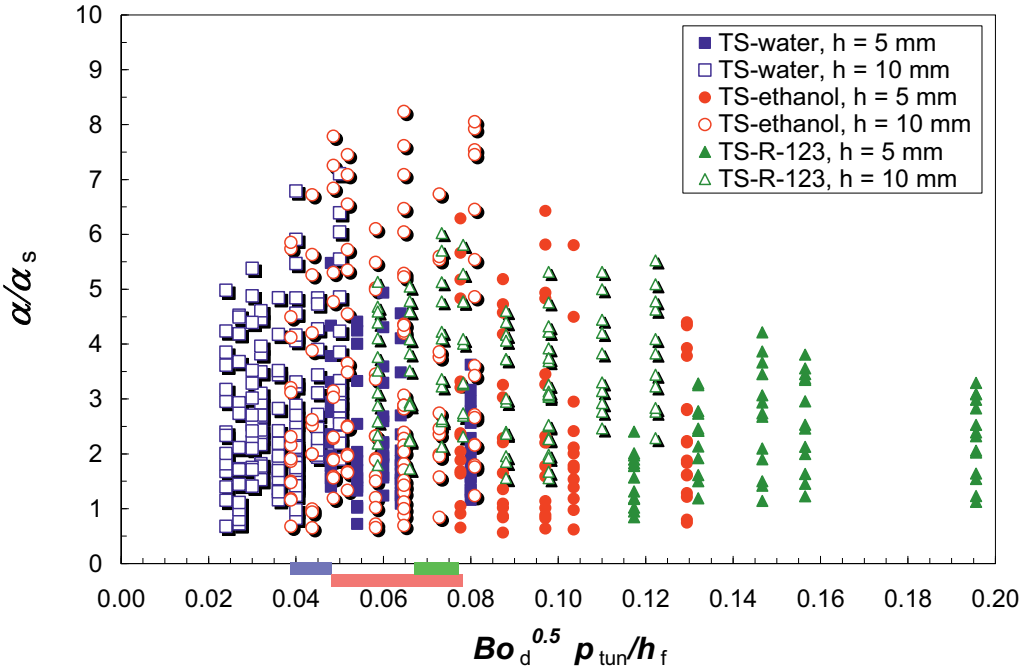

Fig. 5. Generalized results for TS surface.

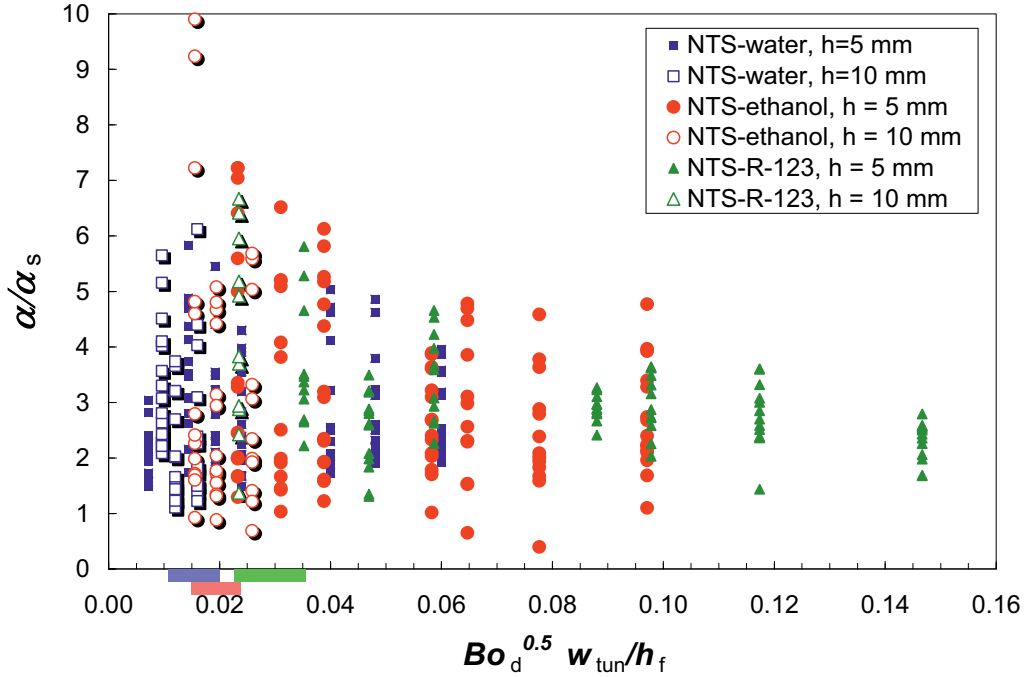

Fig. 6. Generalized results for NTS surface.

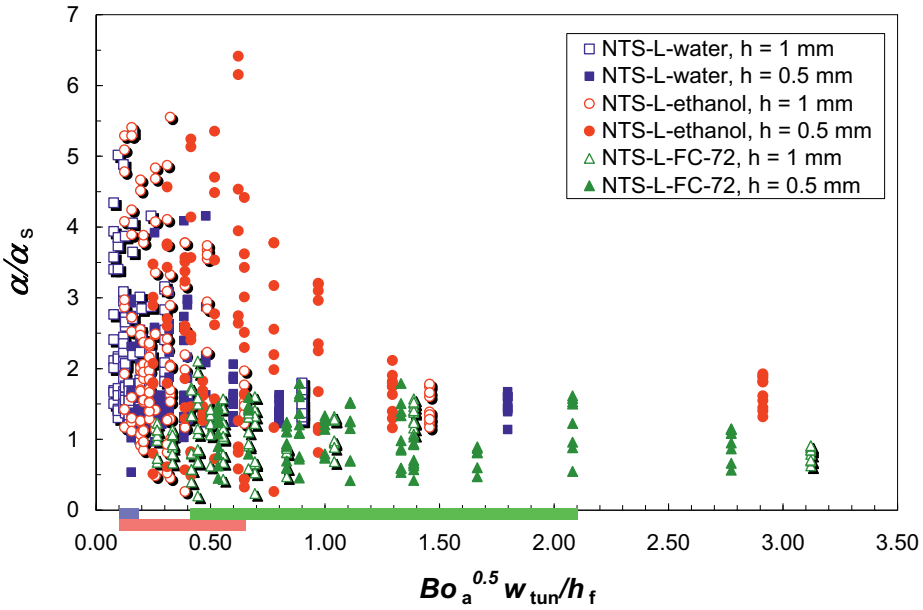

Fig. 7. Generalized results for NTS-L surface.

From the graphs above (figures 5 – 7) it can be concluded that the highest heat transfer coefficients for the particular surfaces are obtained when:

- TS surfaces:

$$0.04 < \left(\mathrm{Bo_d}^{0.5} \frac{p_{\mathrm{tun}}}{h_{\mathrm{f}}} \right) < 0.08 \qquad (7)$$

(water: 0.04 – 0.05, ethanol: 0.05 – 0.08, R-123: 0.07 – 0.08), better results are obtained when the 10 mm high fins are used for all the working fluids.

- NTS surfaces:

$$0.01 < \left(\mathrm{Bo_d}^{0.5} \frac{w_{\mathrm{tun}}}{h_{\mathrm{f}}} \right) < 0.035 \qquad (8)$$

(water: 0.01 – 0.02, ethanol: 0.015 – 0.023, R-123: 0.023 – 0.035), insignificant impact of the fin height change on the α/α_s ratio is observed.

- NTS-L surfaces:

$$0.1 < \left(\mathrm{Bo_a}^{0.5} \frac{w_{\mathrm{tun}}}{h_{\mathrm{f}}} \right) < 2.1 \qquad (9)$$

(water: 0.1 – 0.16, ethanol: 0.1 – 0.65, FC-72: 0.4 – 2.1).

For boiling water the increase in the heat transfer value is reached for h_f = 1 mm. With ethanol and 1 mm high mini-fins, lower values of $\mathrm{Bo_d}^{0,5}$ w_{tun} / h_f are more advantageous. Higher values should be selected in the case of 0.5 mm mini-fins. For FC-72, a minimal effect of the mini-fin height change on the heat transfer coefficient increase is observed.

4 Conclusions

To obtain the highest possible increase in the pool boiling heat transfer coefficient value on the surfaces, it is necessary to properly match the geometrical dimensions of the tunnels and the diameters of the pores or mesh apertures with the characteristic capillary dimension.

The following detailed conclusions can be drawn:

- The TS surfaces help obtain the increase in the heat transfer coefficient value eight times higher than that of the smooth and flat surface, with advantageous average values of (d / L) (p_{tun} / h_f), that is, 0.06 ±0.02.
- The boiling heat transfer coefficients obtained from the NTS surfaces were even 10 times higher than those for the smooth surface. Low values of (d / L) (w_{tun} / h_f) should be used for the best result, that is, 0.02 ±0.01.
- For the boiling of water, ethanol and FC-72 on the NTS-L surfaces, the most advantageous surface geometry depends on the working fluid used. The 3.5-fold decrease in capillary dimension L (when FC-72 is used instead of water) requires about 10-fold increase in (d /L) (w_{tun} / h_f).

References

1. R. Pastuszko, Exp. Thermal Fluid Science **32,** 1564-1577 (2008)
2. R. Pastuszko, Exp. Thermal Fluid Science **38**, 149-164 (2012)
3. R. Pastuszko, EPJ Web of Conferences **45,** 01020 (2013)
4. R. Pastuszko, M. Piasecka, Journal of Physics: Conference Series **395,** 012137 (2012)
5. A. Faghri, *Heat Pipe Science and Technology* (1995)
6. M. S. El-Genk, J. L. Parker, ‚Energy Conversion and Management, **49**, 733-750 (2008)
7. J. R. Thome, *Enhanced Boiling Heat Transfer* (1990)